UDC 617.52;.528

Ye. Kuzenko, A. Romaniuk
Medical institute of Sumy state university

IDENTIFICATION OF EPULIS PATIENTS WITH A HIGH RISK OF PERIODONTAL DISEASES: DNA INFRARED SPECTRA, EXPRESSION MGMT AND P53 BY AND APOPTOSIS ANALYSIS

The objective of this study was to epulis apoptosis analyze, expression of MGMT and p53, DNA methylation patients with a high risk of developing bone resorption and inflammatory periodontal diseases.

Human epulis benign were assessed for their ability to expression of MGMT, p53. 51 epulis DNA were compared by infrared spectroscopy for their ability to apoptosis induced. We conducted a comparative analysis of global expression changes in human epulis using K-S test and Student method.

MGMT and p53 was expressed in giant-cell. Expression of MGMT and p53 in giant-cell epulis. By immunohistochemistry, (97.1±0.42)% ($p<0.001$) of giant-cells were positive for MGMT, whereas only (6.21±0.26)% of giant-cells were positive for p53 ($p<0.001$). Induction of the enzymatic activity of MGMT was increased p53. This could be explained by the fact that MGMT is physiologically expressed by the giant-cell of epulis, p53 expression is weak or absent in giant-cell epulis and non induced apoptosis in the fibrous connective tissue.

Significant changes were observed IR absorption bands at – дsSN3 group bases. In intact periodontium in CH_3 – IR bands were unchanged. Center band oscillations – дsSN$_3$ group was at (1375±1) cm^{-1}. Percentage intensity on a scale transmission of infrared radiation was (7,18±0,74)%. Percentage of infrared absorption bands (1375±1) cm^{-1} in giant cell epulis equal to (13,24±3,7)% (**p = 0.01).

Changes in IR absorption bands observed in дsCH$_2$ group. In intact periodontal дsCH2 next strip – strip center fluctuations – 1464 cm^{-1}, the percentage of intensity on a scale transmission of infrared radiation (0,24±0,03) %. Percentage of IR absorption bands – 1464 cm^{-1} in the giant cell epulis was (0,46±0,09) % (*p = 0.05). Percent transmittance intensity on a scale stretching, deformation and rocking vibrations of CH_3 and CH_2 groups of DNA. Aim of this study was to find if IR can be used in neoplasm process DNA methylation detection. Statistical analysis shows that there are differences between spectra of giant cell epulis and control group. Fitting analysis allows to follow small changes in spectra CH_3 groups. Presented results prove that infrared spectroscopy could be useful tool in DNA methylation. Morphologically, apoptosis is characterized by DNA fragmentation and formation of apoptotic. DNA CH_3 groups can be detected by infrared spectra leads of breaks in DNA strands. This leads to the activation of apoptosis via p53 and MGMT.

Key words: *MGMT and p53, immunohistochemistry oral epulis.*

Gingivitis represents a spectrum of diseases whose origin is commonly attributed to the presence of bacteria, but there are other forms of gingivitis that are not primarily plaque-related. Colonization of periodontal tissues gram-positive and gram-negative periodontal bacteria including: P. gingivalis, Actinomycetemcomitans, T. forsythia, T. denticola, B. Forsythus, P. Gingivalis, F. Nucleatum, P. intermedius, P. nigrescens, and P. micros, S. Sanguis, S. oralis, S. mitis, S. gordonii, S. intermedius, Capnocytophagia, C. concius and E. corrodens appears to be the primary initiator of the disease [1]. Many oral bacteria, the ability to invade periodontal tissues cells and establish an intracellular space is a critical survival mechanism. As exemplified by P. gingivalis, this initially innocuous relationship with a periodontal cell can potentially shift to a more worse [2].

Plaque bacteria evoking the chronic inflammatory response in periodontal tissues [3]. At the same time, it was reported that destructive processes responsible for periodontal tissue breakdown, leading to the clinical of periodontitis [4]. Therefore, the characteristic features of

chronic periodontitis occur mainly as a result of activation of the host-derived immune and inflammatory defense mechanism.

Systemic diseases such as diabetes and leukemia can exacerbate plaque-associated gingivitis, as can endocrine changes (puberty, pregnancy), medications (nifedipine, cyclosporineand phenytoin) and malnutrition (vitamin C deficiency) [5].

Epulis – these overgrowths induced by chronic inflammatory. Kramer's investigation is a convincing periapical irritation induce periodontal disease [6]. In severe cases it's associated with loss of alveolar crest bone. However this is uncommon and it's only confined to the soft tissue. More common in female probably due to hormonal defect, most affected area is anterior to molar teeth [7]. Now epulides can be classified (according to clinical appearance, histopathologic appearance and sometimes the origin) into fibrous epulis, ossificans epulis, pyogenic granuloma (also known as, angina epulis, hemangioma), giant cell epulis (also known as osteoclastoma, giant cell reparative granuloma, peripheral giant cell granuloma or giant cell hyperplasia) and combined epulis.

Specific T- and B-cell–mediated antibacterial responses activate a network of regulatory cytokines (IFNG gene) that are produced by infiltrating T-helper type. The methylation pattern of the promoter region CpG from the IFNG gene have studed Kelma Campos et al. 2013 [8]. Bobetsis et al [9] presented partial or total methylation of the promoter region of the gene IFNG that is epigenetic alteration during inflammatory.

IFNG gene in experimentally induced gingivitis independent of promoter methylation alteration. Hypomethylation IFNG gene promoter region is related to an increase of IFNG transcription present in the chronic periodontitis biopsies [10].

A study by Yin and Chung [11] says that bacterial infection (Campylobacter rectus) induced hypermethylation of the placental f2 promoter of mice. It is well accepted that exposure to different oral bacteria results in differential methylation profiles. Recent evidence indicates that changes related to methylation patterns can occur in periodontitis.

The hypermethylation of E-cadherin, COX-2 and PTGS-2 genes have described in gingival biopsy samples from individuals with chronic periodontitis [12, 13]. Other studies [14, 15] have suggested that the hypomethylation of IL-8 gene is present in oral epithelial cells from individuals with aggressive periodontitis and with chronic periodontitis.

In [16] there was a discuss about hypermethylation status of E-Cadherin and COX-2 genes. Wings TY Looet al [16] analysis shown correlated among the three groups with statistical significance ($p < 0.0001$). The methylation of CpG islands in E-Cadherin and COX-2 genes in periodontitis patients occurs more frequently in periodontitis patients than in thecontrol subjects, but occurs less frequently than in the breast cancer patients.

Hypermethylation in the IFN-г and IL-10 genes B.V. Michelle et al. is a first time investigated in healthy and inflamed periodontal tissues [17].

In recent years, our understanding of the processes controlling the dynamics of partial methylation of IL-6 gene has been considerably investigated by Florenc Abdanur Stefani et al. [18].

The overall methylation of the studied PTGS2 promoter region (-541 bp ~ -216 bp) in chronically inflamed gingival tissues has 5.06-fold higher than the methylation level exhibited in non-inflamed gingival tissues [19].

The results F.P. Naila et al indicate that individuals with chronic periodontitis, independent of smoking habit, have a higher percentage of hipomethylation of the IL8 gene than those controls in epithelial oral cells ($p=0.0001$), and expression of higher levels of interleukin-8 (IL-8) mRNA than controls in gingival cells. F.P. Naila et al has conclude that inflammation in the oral mucosa might lead to changes in the DNA methylation status of the IL8 gene in epithelial oral cells [20].

The most dangerous endogenous DNA methylating agent is S-adenosylmethionine (SAM) [21]. SAM is a coenzyme involved in more than 40 metabolic reactions transfer of methyl groups on nucleic acids [22]. On the one hand, enzymatic DNA methylation is necessary for the regulation of gene expression, on the other hand – can lead to mutagenesis of DNA [23].

During the marginal periodontitis inflammation in the cell SAM able to create: thousand 7-Methylguanosine (m7G), hundreds – 3 methyladenine (m3A) and tens – of Methylguanosine 6th (m6G) [24]. The first two adduct contribute to the formation of AP sites or blocking DNA replication.

MGMT protein acts through a self-destruction mechanism, removing abnormal adducts

from the O6 position of guanine, providing protection from mutagenic agents [25]. Loss of MGMT expression has been associated with aggressive tumor behavior and progression in several types of neoplasia, including esophageal, hepatocellular, lung, gastric and breast carcinomas [26].

Many types of stress activate p53, including DNA damage, telomere attrition, oncogene activation, hypoxia and loss of normal growth and survival signals. These stress signals may be encountered by a developing tumor. Activation of p53 can induce several responses in cells, including differentiation, senescence, DNA repair and the inhibition of angiogenesis [27].

So it is necessary to understand the cellular mechanism of degeneration in periodontal tissues in various types of epulis. DNA methylation under the influence of chronic inflammatory could be key to better understand disease evolution.

In the present work, we show the expression of MGMT and p53 in epulis. There have been no reports about expression of MGMTand p53 in various types of epulis.

Methods. The study sample consisted of periodontal and epulis tissues of patients. The subjects were divided into two equal groups:

• patient's group (group I): included 51 people who had clinical diagnosis of epulis. Only patients with available tissue represent a subset of the overall study groups;

• control group (group II): included 9 patients who died in Sumy Regional Hospital Patients with various diagnoses (not atherosclerotic ones).

Ethics statement. All study and family the deceased participants were informed about the study and those who agreed to participate signed a consent form. Ethical approval for conducting the study was obtained from the Health Ministry of Ukraine (HMU). Approval for performing oral examination was obtained from the authorities of the respective hospital and clinic. Information about the biopsy made in medical records and postmortem epicrisis Patients who agreed to take part on a surveillance confidential study, in accordance to the Local Research Ethics committee from medical institute of Sumy State University, Sumy Ukraine, approved under the number 013U003315, were enrolled in this study.

The infrared spectroscopy was used for gathering structural information on biological systems, but not used in periodontitis inflammation researchers. The study of DNA by infrared spectroscopy requires peeled DNA samples. The infrared specters of DNA show many characteristic: denaturation, alkylation, dehydration and conformational transition.

DNA was isolated from epulis and periodontal tissues using buffer (30 mMTrisCl; 10 mM EDTA; 1 % SDS; proteinaza-K). DNA purification was performed standard phenolic-chloroform method followed by precipitation in absolute ethanol. The resulting DNA product was triturated with and embedded in KBr tablet subsequent FTIR spectrophotometer Spectrum One (Perkin Elmer).

Hematoxylin and eosin (H&E) stains have been used for at least a century and are still essential for recognizing various tissue types and the morphologic change. Paraffin sections are immersing into three sets of xylene for 10 minutes each followed by three sets of absolute ethanol for 10 minutes and finally rinsed with tap water. Slides are placed into haematoxylin for 5 minutes and rinsed thoroughly under tap water for approximately 4–5 minutes. Excess haematoxylin is removed by adding 1 % acid alcohol (1 % HCl in 70 % (v/v) alcohol) for 5 seconds followed by a tap water wash. The slides are rinsed in tap water before being stained in eosin (1 % (w/v) for 15 seconds with a subsequent wash in running tap water for 1–5 minutes. The slides are covered with glass cover slips.

Paraffin sections were prepared for acridine orange staining by mounting on superfrost slides, drying a hot plate, and then immersing into three sets of xylene for 2 minutes each followed by three sets of absolute ethanol for 5 minutes and finally rinsed with tap water. The aim was to remove the wax and dehydrate the sections. Slides (paraffin) were placed into acridine orange staining solution for 15 minutes, and rinsed with phosphate-buffered saline (PBS). Then the slide was soaked in 0.1 % calcium chloride solution for 3 minutes and was washed with PBS once again. Cover glass was mounted for observation under a fluorescence microscope to observe and read the result.

Immunostainings for MGMT and p53 were performed on formalin-fixed (pH 7,4), paraffin-embedded thyroid tissue sections using mouse monoclonal anti- MGMT, and anti- p53 (Thermo Fisher Scientific UK). Briefly, 4мм thick tissue sections were dewaxed in xylene and were brought to water through graded alcohols. Antigen

retrieval was performed by microwaving slides in 10mM citrate buffer (pH 6.2) for 30 min at high power, according to the manufacturer's instructions. To remove the endogenous peroxidase activity, sections were then treated with freshly prepared 1.0 % hydrogen peroxide in the dark for 30 min at 37 °C temperature. Non-specific antibody binding was blocked using blocking serum. The sections were incubated for 30 min, at 37 °C temperature, with the primaries antibodies against MGMT and p53, diluted 1:100 in phosphate buffered saline (PBS) pH 7.2, after washing 3 times with PBS. Anti-(mouse IgG)–horseradish peroxidase conjugate (1:40 000 dilution) was used for the detection of the MGMT, p53, primaries antibodies, sections were then incubated for 20 min, at 37° C temperature. The colour was developed by DAB.

Appearance of positive factors was detected semiquantitatively by counting of positive structures in visual field (+ – few, ++ – moderate, +++ – numerous, ++++ – abundance positive structures in visual field.

Results were presented as mean values (±SD). The K-S test was used in order to evaluate the normality of the data. Also, the Student method was used to perform simple comparative analysis A value of $p<0.05$ was considered significant.

Results. A total of 51 cases including: 20 fibrous epulis,4 ossificans epulis, 9 pyogenic granuloma, 14 giant cell epulis and 4 combined epulis diagnosed and treated in the surgeon of maxillofacial department in Sumy Regional Hospital and, Sumy Regional Oncology Center Ukraine from 2012 to 2014 were retrospectively analysed. Epulides were classified basing on histopathological diagnosis.

The patients were divided into four age groups, ie., group I – up to 18 years; group II – 18 to 40 years; group III – 41 to 60 years and group IV – over the age of 60.

The microscopic examination of the hematoxylin and eosin stained section shown, a single of tissue with epithelium and underlying fibrous connective tissue stroma (fig. 1).The sections revealed well-circumscribed, fibroblasts, capillaries, edema areas and occasionally there are bone resorption areas. There were also several areas characterised by haemorrhage, underlined by the presence of Fe deposits.

These microscopic features are typical for a pyogenic epulis. Hematoxylin and eosin stained

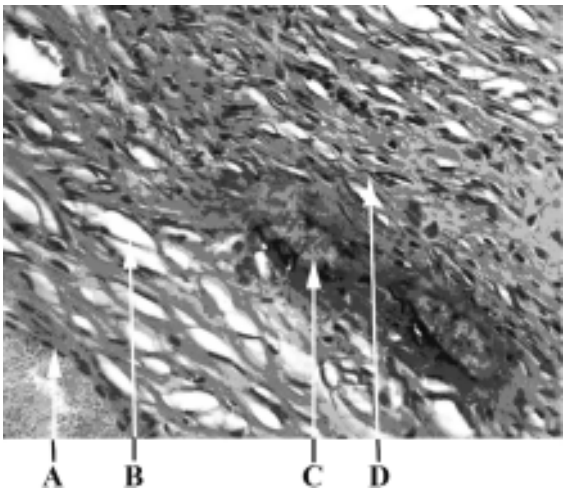

Fig. 1. Fibrous epulis, haematoxylin and eosin (×800):
A – capillaries; B – edema areas, C – resorption areas, D – connective tissue

pyogenic epulis sections of the specimen (fig. 2) exhibited fibrovascular connective tissue with overlying ulcerated stratified squamous epithelium with features of atrophy and proliferation at different places. The ulcerated area was covered by fibrinous exudate. The connective tissue was fibrocellular with abundant vascularity. There were numerous endothelium lined vascular spaces, budding endothelial cells and proliferation of fibroblasts. A moderate degree of chronic inflammatory cell infiltrate, composed chiefly of lymphocytes and plasma cells, was present.

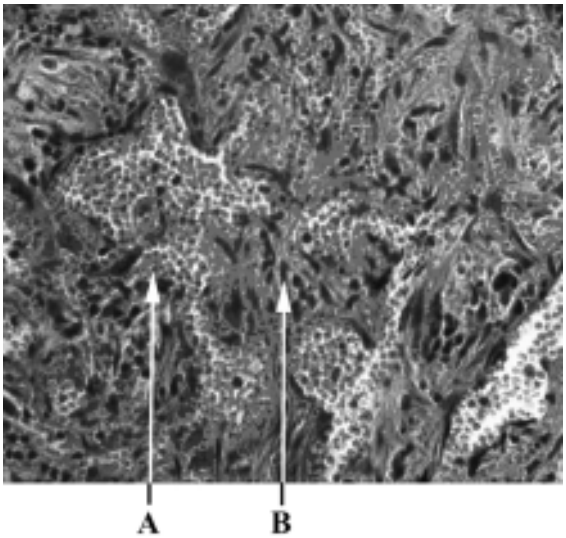

Fig. 2. Pyogenic epulis, haematoxylin and eosin (×800):
A – vascular spaces**,** B – connective tissue

The sections revealed well-circumscribed, unencapsulated cellular mass containing oval to spindle-shaped fibroblasts, abundant multinucleated giant cells (fig. 3), numerous capillaries (fig. 3 A) and areas of haemorrhage. These giant cells were localized in the deep corion in a vascular stroma of ovoid and spindle shaped fibroblastys. The multinucleated giant cells were of variable shapes and sizes containing open-faced nuclei ranging from 10 to 25 in number conforming to the type I giant cells described in literature. There were also several areas characterized by haemorrhage, underlined by the presence of Fe deposits.

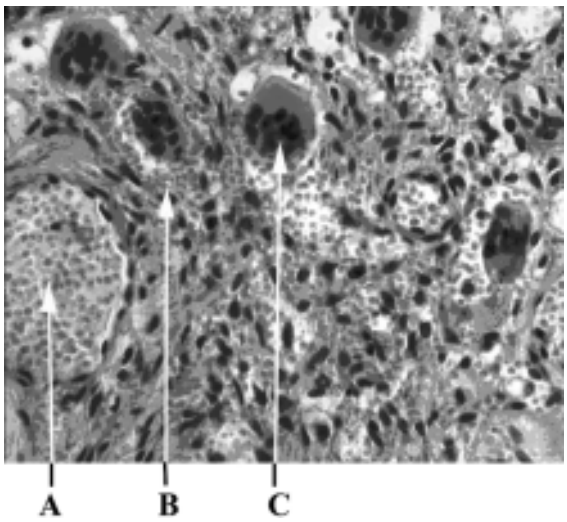

Fig. 3. Giant-cell epulis, haematoxylin and eosin (×400):
A – capillaries, B – areas of haemorrhages, C – giant cells

The diagnosis was ossificans epulis with spindle-shaped fibroblasts (fig. 4). There were no atypias or mitotic figures presence of a fusocellular tumor containing calcifications with concentric and acellular mineralization at the center and other areas presenting recently formed osteoid with peripheral osteoblasts and signs of progressive calcification**.**

MGMT and p53 was expressed in giant-cell. Expression of MGMT and p53 in giant-cell epulises shown in fig. 5 and 6. By immunohistochemistry (97.1±0.42)% ($p<0.001$) of giant-cells were positive for MGMT, whereas only (6.21±0.26)% of giant-cells were positive for p53 ($p<0.001$). Induction of the enzymatic activity of MGMT was increased p53. This could be explained by the fact that MGMT is physiologically expressed by the giant-cell of epulis, p53

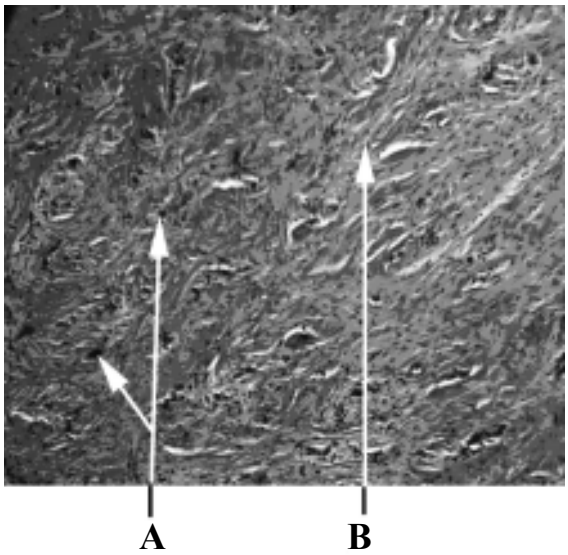

Fig. 4. Ossificans epulis, haematoxylin and eosin (×100):
A – acellular mineralization; B – fibroblasts

expression is weak or absent in giant-cell epulis and non induced apoptosis in the fibrous connective tissue.

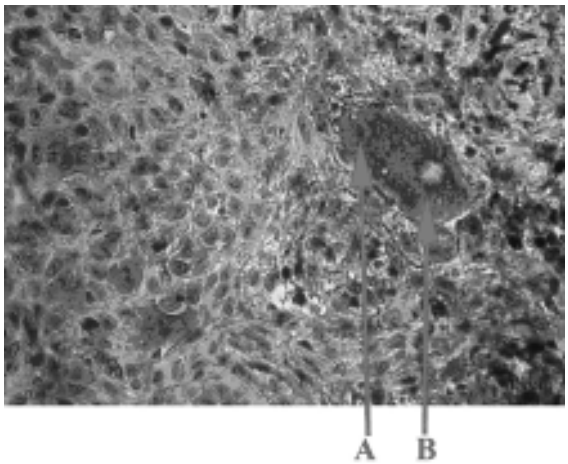

Fig. 5. Expression of MGMT proteins in giant-cell epulis(×800):
A – giant cells MGMT «-» nucleus; B – giant cells MGMT «+» cytoplasm

P53 immunoexpression was negative in the 18 cases of fibrous epulis and positive in the case of simple dysplasia from the papilloma type, confirming the changes noted in usual staining (fig. 7). In all of the fibrous epulis MGMT was positive [(98.54±10.19)%].

Positive MGMT immunostaining was present in (87.2±7.20)% of ossificans epulis. Positive p53 immunostaining was found in (23.00±2.02)% of ossificans epulis.

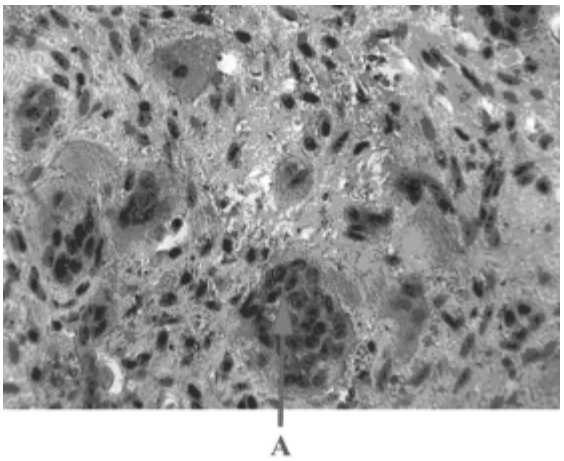

Fig. 6. Expression of p53 proteins in giant-cell epulis, (×800): A – giant cells p53 «-»

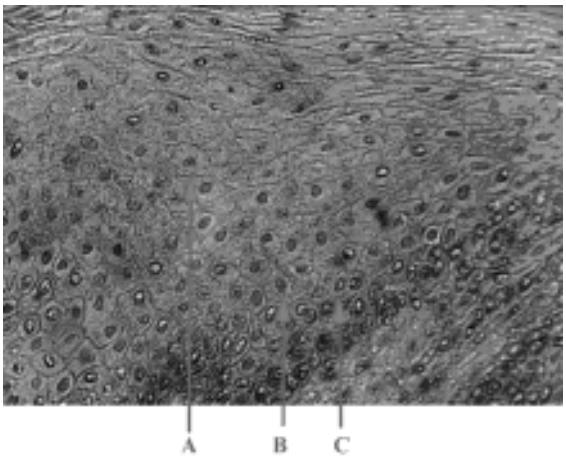

Fig. 7. Expression of p53 proteins indysplasia from the papilloma type (×600): A – cells p53 «-»; B – cells p53 «+»; C – basal cells

All pyogenic epulis immunopositivity for MGMT in fibroblasts and in cellular infiltration. Interestingly, in the periphery of the lesion these ones showed a moderate positivity around the blood vessels to MGMT (24.35±4.89)% related antigen, reaction not evident deeper in the fibroblasts and in cellular infiltration. In 9 of the samples analyzed at least one the p53 sample was positive.

deoxyribose. Stretching vibrations of the C-H fragments alkyl groups CH_3, CH_2 appear in the 3000–2840 cm^{-1}. In the area spectra 3000–2840 cm^{-1} arises partly overlay peaks of adenine, thymine, guanine, cytosine. For differentiation groups CH_3, CH_2, remember that stretching vibrations Ssp3-H bonds are usually observed below 3000 cm^{-1}, while stretching vibrations links Ssp2-N and Ssp-N lie above 3000 cm^{-1} (fig. 8).

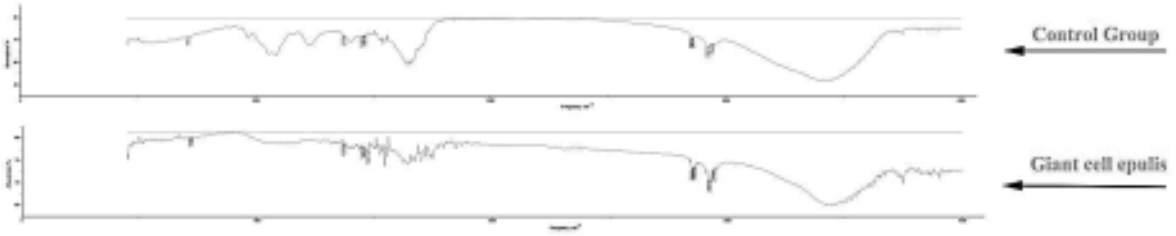

Fig. 8. DNA IR specter

Infrared spectra (IR) of the DNA bands can be roughly divides into three areas: first – 4000–2000 cm-1 – variations of bases, the second – 1700–1500 cm-1 – DNA deoxyribose vibrations, third – 1300–1000 cm-1 – deoxyribose vibrations and phosphate groups in the skeleton of the DNA molecule. The bands of the spectrum depending on the absorption of infrared radiation can be dividedinto: strong – ≤ 20% average – 20 %–5% and weak – 5 % ≥. Due to the complexity of the structure of DNA arises imposition peaks of adenine, thymine, guanine, cytosine, deoxyribose and phosphorus balance in the group CH3, CH2.

The most important differentiation CH3 groups attached to abnormal bases from CH 2 groups

Stretching vibrations of methyl groups (CH_3) are observed as two bands at 2962 and 2872 cm^{-1}.

The first – the result of antisymmetric stretching vibrations in which the two C-H stretching of the methyl group, while the third connectivity is compressed (нas CH_3).

The second band is due to symmetric stretching vibrations (нs CH3), when all three C-H bonds are stretched or compressed in phase. The presence of several methyl groups leads to an increase in the intensity of the respective bands.

Stretching vibrations of methylene groups (CH_2) are also observed in two bands (2962 and 2853 cm^{-1}) due to antisymmetric (нas CH_2) and symmetric (нs CH_2) stretching vibrations.

In the methyl groups may show two deformation vibrations: symmetric deformational vibrations (дs CH_3), which is found around 1375 cm^{-1} and antisymmetric deformational vibrations (дas CH^3) – in the 1450 cm^{-1}.

The absorption at 1375 cm^{-1} is an important criterion (дs CH_3) group. Negligible absorption band in the spectrum of DNA and characterized compression intact DNA. Methyl group has four types of deformation vibrations (scissor, fan-shaped, shuttle, spinning). The most informative is the absorption in the 1465 cm^{-1} due to scissor deformation vibrations (дs CH_2). Therefore, CH_3 and CH_2 comparison groups in DNA intact periodontium and periodontal epulides of the above, we analyze in the absorption band.

Significant changes were observed IR absorption bands at – дsSN_3 group bases. In intact periodontium in CH_3 – IR bands were unchanged. Center band oscillations – дsSN_3 group was at (1375±1) cm^{-1}. Percentage intensity on a scale transmission of infrared radiation was (7,18± 0,74)%. Percentage of infrared absorption bands 1375±1 cm^{-1} in giant cell epulis equal to (13,24± 3,7)% (** p = 0.01).

Changes in IR absorption bands observed in дsCH_2 group. In intact periodontal дsCH_2 next strip – strip center fluctuations – 1464 cm^{-1}, the percentage of intensity on a scale transmission of infrared radiation – (0,24 ± 0,03)%. Percentage of IR absorption bands – 1464 cm^{-1} in the giant cell epulis was (0,46±0,09)% (*p = 0.05).

In most model systems, etoposide-induced apoptosis is dependent on p53 [28]. Acridine orange is a nucleic acid selective metachromatic stain useful for cell cycle determination. Acridine orange interacts with DNA and RNA by intercalation or electrostatic attraction respectively. DNA intercalated acridine orange fluoresces green (525 nm); RNA electrostatically bound acridine orange fluoresces red (>630 nm). It may distinguish between quiescent and activated, proliferating cells, and may also allow differential detection of multiple G_1 compartments. Acridine orange also measuring apoptosis, and for detecting intracellular gradients and the measurement of proton-pump activity (fig. 9). The apoptotic cells were greenish yellow in color whereas the necrotic cells were orange-red. Significant decrease ($p<0.05$) in apoptotic cells was observed among all epulis whereas maximum apoptosis was observed in giant cell epulis on interaction

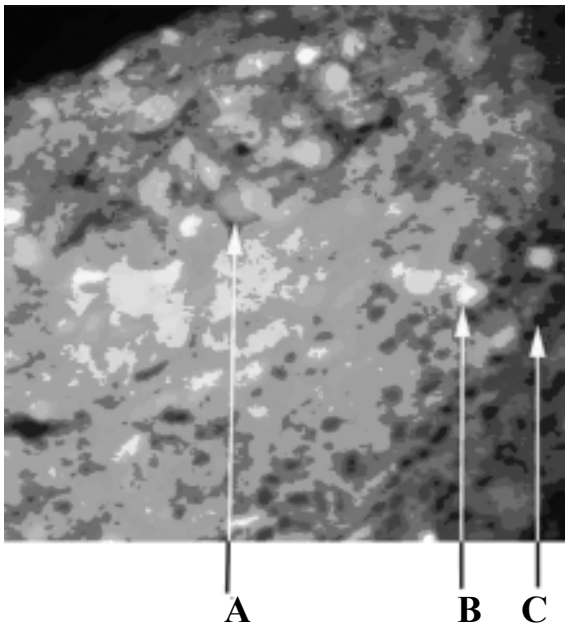

Fig. 9. Giant-cell epulis, acridine orange (×800): A – necrotic cells, B – apoptotic cells, C – erythrocytes

which was confirmed by DNA IR absorption bands (fig. 8).

Discussion. In this study, the expression of MGMT and p53 was examined to elucidate the relationship between their immunostaining. We found that in MGMT cells P53 expression was significantly lower. This is in line with the results of our previous study [29]. Abnormal promoter methylation is not the only determining factor in the regulation of MGMT expression [30.]. Other regulators of MGMT expression must be explored to determine this, and the tumor suppressor p53 may be an interesting candidate.

The determination of mutational spectra has defined two areas of contemporary interest in the role of MGMT in mutation avoidance. The first of these is the issue of sequence and DNA strand-specificity of induced mutation. The second concerns the role of MGMT in protection against spontaneous mutation [31].

The recognition of DNA damage (double-strand) start mechanisms leading to apoptosis by activating p53 gene. P53 gene haz its name from the molecular weight of the protein, encoded by it – p53 kDa inactive in normal cells.Now function of the gene P53 can be classified into: helps cell differentiation, cell cycle regulation, cellular responses to DNA damage, DNA repair, start replication and apoptosis [32].

Abnormal proliferation and various cells damaging is response of activation p53 gene.Cycle cell phase (G1 or G2) stops p53 protein through its target genes. The target gene starts DNA replication before mitosis and stimulates the DNA repair or induces apoptosis. [33, 34]. In addition, the p53 protein itself is involved in DNA repair, inhibits angiogenesis and acts as transcription factor of many genes [35, 36].

Researches of gene expression TP53 and MGMT in different cell types of human tumors is very inconsistent. Mice and rats given conflicting results about the relationship between the expression of these two genes. Some researchers experimentally demonstrated the inhibitory activity of p53 into MGMT expression, other researchers on cell lines showed that the MGMT gene expression inhibits p53 wild-type [37–44]. T. Osanai et al. [45] found that samples of human breast tumors expressing p53 does not inhibit MGMT. Astrocytes cell (mice lines) expressing p53 wild-type have higher activity MGMT [46]. Decreased MGMT expression found in different samples of human tissue in which the observed changes.in p53 [47]. A. Chakravarti et al demonstrated to matched wild-type p53 expression may be necessary for MGMT expression.MGMT and mutant p53 can reduce expression of the genes [48]. Thus, p53 is involved in the regulation of active MGMT. Summing the results of different studies should indicate that p53 is involved in the induction of gene MGMT and protein activity.However, high levels of expression of p53 suppresses promoter activity of MGMT gene [49].

Owing to the high morphological heterogeneity found in tumors, it has been proposed to use the changes in CH_3 and CH_2 absorption ratios to avoid normalization of absorptions [50]. In this way, the data treatment of IR images is faster and does not require spectra manipulation to obtain accurate results. However, owing to the weak absorption changes found for phospholipids submitted to oxidative stress, typically a 5–10 % absorption decrease for nas(CH_2) and a correlative 3–7 % absorption increase in n(CH) [51] is observed – global analysis of tumor mass usually fails to highlight these changes between low-grade tumors, for example, astrocytoma and glioblastoma [52].

Conclusion. Aim of this study was to find if IR can be used in neoplasm process DNA methylation detection. Statistical analysis shows that there are differences between spectra of giant cell epulis and control group. Fitting analysis allows to follow small changes in spectra CH_3 groups. Presented results prove that infrared spectroscopy could be useful tool in DNA methylation. Morphologically, apoptosis is characterized by DNA fragmentation and formation of apoptotic. DNA CH_3 groups can be detected by infrared spectra leads of breaks in DNA strands. This leads to the activation of apoptosis via p53 and MGMT.

References

1. *Feng Z., Weinberg A.* Role of bacteria in health and disease of periodontal tissues. Periodontol. 2006; 40: 50–76.

2. GENA D. TRIBBLE and RICHARD J. LAMONT. Bacterial invasion of epithelial cells and spreading in periodontal tissue. Periodontol. 2000 2010; 52(1): 68-83.

3. *Amano A.* Host-parasite interactions in periodontitis: mi-crobial pathogenicity and innate immunity. Periodontology 2000; 54: 9–14.

4. *Taubman M.A., Valverde P., Han X., Kawai T.* Immune response: the key to bone resorption in periodontal disease. J. International Academy of Periodontology 2005; 76: 2033–2041

5. *Colin B. Wiebe, Edward E. Putnins.* The Periodontal Disease Classification System of the American Academy of Periodontology – An Update. J. Canadian Dental Association 2000; 66 (11): 594–597.

6. *Kramer I.R.H., Pindborg J.J., Shea M.* Histologic typing of odontogenictumours. 2nd ed. Berlin, Springer-Verlag 1992; 118.

7. *Choi C., Terzian E., Schneider R., Trochesset D.A.* Peripheral giant cell granuloma associated with hyperparathyroidism secondary to end-stage renal disease: a case report. J Oral MaxillofacSurg 2008; 66: 1063–66.

8. Carolina Cavalieri Gomes, Jeane de Fatima Correia-Silva. Methylation Pattern ofIFNG in Periapical Granulomas and Radicular CystsKelmaCampos. JOE 2013; 39 (4).

9. *Bobetsis Y.A., Barros S.P., Lin D.M.* Bacterial infection promotes DNA hyperme-thylation. J. Dent Res 2007; 86: 169–74.

10. *Zhang S., Crivello A., Offenbacher S.* [et al.] Interferon-gamma promoter hypomethylation and increased expression inchronic periodontitis. J ClinPeriodontol current year 2010; 37: 953–961.

11. *Yin L., Chung W.O.* Epigenetic regulation of human β - defensin 2 and CC chemokine ligand 20 expression in gingival epithelial cells in response to oral bacteria. Mucosal Immunol 2011; 4:409–19.

12. *Loo W.T., Jin L., Cheung M.N.* Epigenetic change in E-cadherin and Cox-2 to predict chronic periodontitis. J. Trans. Med. 2010; 8:110.

13. *Zhang S., Barros S.P., Niculescu M.D.* [et al.]. Alteration of PTGS2 promoter methylation in chronic periodontitis. J. Dent. Res. 2010; 89 (2): 133–137.

14. *Oliveira N.F.P., Damm G.R., Andia D.C.* [et al.]. DNA methylation status of IL-8 gene promoter in oral cells of smokers and nonsmokers with chronic periodontitis. J. Clin. Periodontol 2009; 36: 719–725.

15. *Andia D.C., de Oliveira N.F., Casarin R.C.* [et al.]. DNA methylation status of the IL-8 gene promoter in aggressive periodontitis. J. Periodontol 2010; 81 (9): 1336–1341.

16. *Wings T.Y. Loo, Lijian Jin, Mary N.B.* Epigenetic change in E-Cardherin and COX-2 to predict chronic periodontitis. Cheung J. Transl. Med. 2010; 8:110.

17. *Michelle Beatriz Viana, Fabiano Pereira Cardoso, Marina Goncalves.* Methylation pattern of IFN-γ and IL-10 genes in periodontal tissues. DinizImmunobiology 2011; 216: 936- 941.

18. *FlorencAbdanur Stefani, Michelle Beatriz Viana, Ana Carolina.* Expression, polymorphism and methylation pattern of interleukin-6 in periodontal tissues. DupimaImmunobiology 2013.

19. *Zhang S., Barros S.P., Niculescu M.D.* Alteration of PTGS2Promoter Methylation in chronic Periodontitis. J DENT RES 2010; 89: 133.

20. *Naila F.P., Oliveira, Gilcy R,Damm* [et al.]. DNA methylation status of theIL8 gene promoter in oral cells of smokers and non-smokers with chronic periodontitis. Clin. Periodontol. 2009; 36: 719–725.

21. *Tchantchou F., Graves M., Ortiz D.* S-adenosylmethionine:A connection between nutritional and genetic risk factors for neurodegeneration in Alzheimer's disease. J. Nutr Health Aging 2006; 10 (6): 541–545.

22. *Feng Yan, Jacqueline M. LaMarre, ReneRohrich.* RlmN and Cfr are radical SAM enzymes involved in methylation of ribosomal RNA.J. Am. Chem. Soc. 2010; 132 (11): 3953–3964.

23. *Sudhakar Veeranki, Suresh C Tyagi.* Sudhakarveeranki defective homocysteine metabolism: potential implications for skeletal muscle malfunction. International Journal of Molecular Sciences 2013; 14: 15074–15091.

24. *Janice R. Sufrin, Steven Finckbeiner, Colin M.* Marine-Derived Metabolites of S-Adenosylmethionine as Templates for New Anti-Infectives. Oliver Marine Drugs 2009; 7: 401–434.

25. *Karran P., Bignami M.* Self-destruction and tolerance in resistance of mammalian cells to alkylation damage. Nucleic Acids Research, 2009; 20(12): 2933 –2940.

26. *Giaginis C., Michailidi C., Stolakis V.* [et al.]. Expression of DNA repair proteins MSH2, MLH1 and MGMT in human benign and malignant thyroid lesions: An immunohistochemical study. Med Sci Monit. 2011, 17 (3): 81–90.

27. *Kevin M. Ryan, Andrew C. Phillips, Karen H.* Regulation and function of the p53 tumor suppressor protein.Vousden Current Opinion in Cell Biology 2001, 13: 332–337.

28. *Karpinich N.O., Tafani M., Rothman R.J.* [et al.]. The course of etoposide-induced apoptosis from damage to DNA and p53 activation to mitochondrial release of cytochrome c. J. Biol. Chem 2002; 277: 16547–16552.

29. *Kuzenko Y., Romanyuk A.* Giant-cell epulis: immunohistochemical analysis of MGMT, p53, OPN and MMP-1.Osteologicky bulletin 2013; 18(3):87–9.

30. *Brell M., Tortosa A., Verger E.* [et al.]. Prognostic significance of O6-methylguanine-DNA methyltransferase determined by promoter hypermethylation and immunohistochemical expression in anaplastic gliomas. Clin Cancer Res 2005; 11: 5167–5174.

31. *Karran P., Bignami M.* Self-destruction and tolerance in resistance of mammalian cells to alkylation damage. Nucleic Acids Research, 2013; 20(12): 2933–2940.

32. *Giarnieri E., Mancini R., Pisani R.* [et al.]. Msh2, Mlh1, Fhit, p53, Bcl- 2 and Bax expression in invasive and in situ squamous cell carcinoma of uterine cervix. Clin. Cancer Res. 2000; 9: 3600-6.

33. *Vogelstein B.* p53 function and dysfunction. KW Kinzler 1992;70(4): 523–526.

34. *Liebermann D.A., Hoffman B., Steinman R.A.* Molecular controls of growth arrest and apoptosis: p53-dependent and independent pathways. Oncogene 1995; 11(1): 199–210.

35. *Albrechtsen N., Dornreiter I., Grosse F.* Maintenance of genomic integrity by p53: complementary roles for activated and non-activated p53. Oncogene 1999;18(53):7706–7717.

36. *Semin W.S. el-Deiry.* Regulation of p53 downstream genes. Cancer Biol 1998;8 (5): 345–357.

37. Harris L.C., Remack J.S., Houghton P.J., Brent T.P. Wild-type p53 suppresses transcription of the human O6-methylguanine-DNA methyltransferase gene. Cancer Res 1996;56(9): 2029–2032.

38. *Wolf P., Hu Y.C., Doffek K.* [et al.]. O (6)-methylguanine-DNA methyltransferase promoter hypermethylation shifts the p53 mutational spectrum in non-small call lung cancer. Cancer Res 2001;61(22): 8113–81117.

39. *Osanai T., Takagi Y., Toriya Y.* [et al.]. Inverse correlation between the expression of O6 - methylguanine-DNA methyltransferase (MGMT) and p53 in breast cancer. Jpn. J. Clin. Oncol. 2000; 35(3): 121–125.

40. *Kaina B., Ziouta A., Ochs K., Coquerelle T.* Chromosomal instability, reproductive cell death and apoptosis induced O6-methylguanine-DNA in Mex-, Mex + and methylation-tolerant mistmatch repair compromised cells: facts and models. Mutant. Res 1997;381(2): 227–241.

41. *Bean C.L., Bradt C.I., Hill R.* [et al.]. Chromosome aberrations: persistence of alkylation damage and modulation by O6 - alkylguanine-DNA alkyltransferase. Mutat.Res 1994; 307(1): 67–81.

42. *Debiak M., Nikolova T., Kaina B.* Loss of ATM sensitizes against O6 - methylguanine triggered apoptosis, SCEs and chromosomal aberrations. DNA Repair (Amst) 2004; 3(4) :359–368.

43. *Kaina B., Fritz G., Coquerelle T.* Contribution of O6-alkylguanine and N-alkylpurines to the formation of sister chromatid exchanges, chromosomal aberrations, and gene mutations: new insights gained from studies of genetically engineered mammalian cell lines.Environ. Mol> Mutagen 1993; 7(5): 1398–1409.

44. *Srivenugopal K.S., Shou J., Mullapudi S.R.S.* [et al.]. Enforced expression of wild-type p53 curtails the transcription of the O6-methylguanine-DNA methyltransferase gene in human tumor cells and enhances their sensitivity to alkylating agents. Clinical Cancer Res 2001; 7(5): 1398–1409.

45. *Osanai T., Takagi Y., Toriya Y.* [et al.]. Inverse correlation between the expression of O6 - methylguanine-DNA methyltransferase (MGMT) and p53 in breast cancer.Jpn. J. Clin. Oncol. 2008; 35(3): 121–125.

46. *Nutt C.L., Loktionova N.A., Pegg A.E.* [et al.]. O6 - methylguanine-DNA methyltransferase activity, p53 gene status and BCNU resistance in mouse astrocytes. Carcinogenesis 1999; 20(12): 2361–2365.

47. *Rolhion C., Penault-Llocra F., Kemeny J.L.* [et al.]. O6 - methylguanine-DNA methyltransferase gene (MGMT) expression in human glioblastomas in relation to patient characteristics and p53 accumulation. Int. J. Cancer 1999; 84(4). 238–245.

48. *Chakravarti A., Erkkinen M.G., Nestler U.* Temozolomide-mediated radiation enhancement in glioblastoma: areportonunderlyingmechanisms. Clin. Cancer Res 2006;12(15): 4738–4746.

49. *Grombacher T., Eichhorn U., Kaina D.* p53 is involved in regulation of the DNA repair gene O6 - methylguanine-DNA methyltransferase (MGMT) by DNA damaging agents. Oncoegene 1998; 17(7): 845–851.

50. *Petibois C., Derlerris G.* Oxidative stress effects on erythrocytes determined by FT-IR spectrometry. Analyst 2004;129: 912–916.

51. *Petibois C., Derlerris G.* FT-IR spectrometry utilization for determining changes in erythrocyte susceptibility to oxidative stress.Progr. Biomedical Optics Imaging 2004; 5: 26–35.

52. *Beleites C.* Classification of human gliomas by infrared imaging spectroscopy and chemometric image processing.Vib. Spectrosc 2005.

Е.В. Кузенко А.М. Романюк

ИССЛЕДОВАНИЯ ЭПУЛИСОВ ПАЦИЕНТОВ С ВЫСОКИМ РИСКОМ ЗАБОЛЕВАНИЙ ПАРОДОНТА МЕТОДАМИ ДНК-ИНФРАКРАСНОЙ СПЕКТРОФОТОМЕРИИ, ИММУНОГИСТОХИМИИ (MGMT И P53) И ЛЮМИНЕСЦЕНТНОЙ МИКРОСКОПИИ

Проанализированы морфологические особенности разных типов эпулиса, апоптоз, уровень экспрессии MGMT и p53, метилирование ДНК у пациентов с воспалительными заболеваниями пародонта. Ткани эпулиса оценивали морфологически и по уровню экспрессии белков MGMT и p53. Уровень метилирования ДНК 51 эпулиса оценивали с помощью инфракрасной спектроскопии, а способность к апоптозу – окраской акридиновым оранжевым.

Экспрессия белков MGMT и p53 выражена в гигантских клетках. Иммуногистохимически в гигантских клетках MGMT была положительной (97,1 ± 0,42) %, p<0,001, в то время как только ядра p53 гигантских клеток были положительными (6,21 ± 0,26) %, p<0,001. Экспрессия MGMT была больше, чем экспрессия p53. Это можно объяснить тем, что MGMT является репаративным ферментом. Изменения полос инфракрасного поглощения ДНК гигантоклеточного эпулиса наблюдаются в группе δsCH_2. В грануляционной ткани δsCH_2 центр – 1464 $см^{-1}$ интенсивность по шкале поглощения инфракрасного излучения составила (0,31 ± 0,04) %; полос инфракрасного поглощения – 1464 $см^{-1}$ в ДНК гигантоклеточном составил (0,46 ± 0,09) %, p = 0,05. Увеличение δsCH_3 групп ДНК эпулисов изменяется и имеет следующее направление: фиброзный эпулис → оссифицирующий эпулис → грануляционная ткань → смешанный эпулис → ангиоматозный эпулис → гигантоклеточный эпулис.

Обнаружено эпигенетическое метилирование ДНК. Статистический анализ показывает, что существуют различия между спектрами ДНК гигантоклеточного эпулиса и ДНК контрольной группы. Инфракрасная спектрофотометрия позволяет утверждать об изменении в ДНК с присоединением CH_3 групп. Сделан вывод, что инфракрасная спектроскопия может быть полезным методом исследования в изучении метилирования ДНК.

Ключевые слова: *эпулис, апоптоз, метилирование ДНК.*

Є.В. Кузенко, А.М. Романюк

ДОСЛІДЖЕННЯ ЕПУЛІСІВ ПАЦІЄНТІВ З ВИСОКИМ РИЗИКОМ ЗАХВОРЮВАНЬ ПАРОДОНТА МЕТОДАМИ ДНК-ІНФРАЧЕРВОНОЇ СПЕКТРОМЕТРІЇ, ІМУНОГІСТОХІМІЇ (MGMT І P53) І ЛЮМІНЕСЦЕНТНОЇ МІКРОСКОПІЇ

Проаналізовано морфологічні особливості різних типів епулісів, апоптоз, рівень експресії MGMT і p53, метилювання ДНК у пацієнтів із запальними захворюваннями пародонта. Тканини епулісів оцінювали морфологічно і за рівнем експресії білків MGMT, p53. Рівень метилювання ДНК 51 епулісу оцінювали за допомогою інфрачервоної спектроскопії, а здатність до апоптозу – забарвленням акридиновим оранжевим.

Експресія білків MGMT і p53 виражена в гігантських клітинах. Імуногістохімічно в гігантських клітинах MGMT була позитивною – (97,1 ± 0,42) %, p<0,001, у той час як тільки ядра p53 гігантських клітин були позитивними (6,21 ± 0,26) %, p <0,001. Експресія MGMT була більше, ніж експресія в p53. Це можна пояснити тим, що MGMT є репаративним ферментом.

Зміни смуг інфрачервоного поглинання ДНК гігантоклітинних епулісів спостерігаються в групі δsCH_2. У грануляційній тканині δsCH_2 центр – 1464 $см^{-1}$ інтенсивність за шкалою поглинання інфрачервоного випромінювання склала (0,31 ± 0,04) %; смуг інфрачервоного поглинання – 1464 $см^{-1}$ в гігантоклітинному епулісі – (0,46 ± 0,09) % (p = 0,05). Кількість δsCH_3 груп в ДНК досліджуваних епулісів збільшується і має наступний напрямок: фіброзний епуліс → осифікуючий епуліс → грануляційна тканина → змішаний епуліс → ангіоматозний епуліс → гігантоклітинний епуліс.

Виявлено епігенетичне метилування ДНК. Статистичний аналіз показує, що існують відмінності між спектрами ДНК гігантоклітинного епулісу і ДНК контрольної групи. Інфрачервона спектрофотометрія дозволяє стверджувати про зміну в ДНК з приєднанням CH_3 груп. Зроблено висновок, що інфрачервона спектроскопія може бути корисним методом дослідження у вивченні метилування ДНК.

Ключові слова: *епуліс, апоптоз, метилування ДНК.*

Поступила 22.05.14